Nature of the repulsive Coulomb barrier in multiply charged negative ions

A. Dreuw* and L. S. Cederbaum
Theoretische Chemie, Physikalisch-Chemisches Institut, Universität Heidelberg, Im Neuenheimer Feld 229, 69120 Heidelberg, Germany
(Received 14 July 2000; published 30 November 2000)

The repulsive Coulomb barrier (RCB) for electron emission is a general property of multiply charged anions. When an electron is emitted from a multiply charged anion, the electron experiences short-range attraction by the nuclei and long-range repulsion from the remaining negatively charged system, giving rise to the RCB. Although the RCB is dominated by the electrostatic forces present, it is argued that the exact potential the electron experiences is nonlocal and energy dependent. The theory of the RCB is outlined and related to the theory of Green's functions. Since it is complicated to compute a nonlocal and energy-dependent potential, approximation schemes are introduced that allow convenient calculation of local energy-independent RCB potentials. Three approximation schemes of complementary nature are proposed. The physical meaning of these schemes, the underlying approximations, and their possible weaknesses are discussed in detail. The local approximation schemes are used to calculate the RCB of atomic dianions F^{2-} and O^{2-} and of the linear carbon cluster dianions ${C_n}^{2-}$ $(n=2,4,6,8)$. The atomic dianions serve as convenient objects to study the basis-set dependence of the local approximation schemes. The computed local potentials of the carbon dianions are used to calculate their lifetimes in the framework of Wentzel-Kramer-Brillouin theory. We found that the lifetime of the linear carbon dianions grows markedly when going from ${C_2}^{2-}$ to ${C_8}^{2-}$, and that the latter should be the only species observable in a mass spectrometer. This agrees with the available experimental findings.

DOI: 10.1103/PhysRevA.63.012501 PACS number(s): 33.15.−e

I. INTRODUCTION

When an electron is detached from a neutral atom or molecule a positively charged ion is formed, and thus the interaction between the outgoing electron and the residual cation is attractive due to their strong Coulomb attraction. Detachment of a singly charged anion results in an electron and a residual neutral system, whose long-range interactions are usually weak but also mainly attractive in nature. The situation is different for detachment of multiply charged anions. When an electron is detached from a multiply charged anion the residual system is still negatively charged and, therefore, the long-range interaction between the outgoing electron and this system is dominated by electrostatic repulsion. Combining this long-range electrostatic repulsion with the short-range binding energy of the electron, a repulsive Coulomb barrier (RCB) emerges which has to be passed by the outgoing electron during its detachment process.

The existence of a repulsive barrier can also be rationalized from the different point of view of electron scattering from a negatively charged target, a point of view that will play a role in the present work. Being spatially far away from the target, the projectile electron experiences only the total charge of the target, which is negative. Since the long-range interaction is mainly electrostatic repulsion, the potential energy increases as the electron approaches the target. From a certain distance on, the electrostatic attraction between the nuclei of the target and the scattered electron overcomes this repulsion, and the potential energy of the system decreases. Combining the long-range repulsion and short-range attraction, the scattering potential that the electron experiences is a repulsive Coulomb barrier.

Repulsive Coulomb barriers play a role in other processes as well, for instance, in α decay of nuclei (see, for example, [1]). An α particle that departs from a radioactive nucleus experiences a potential barrier analogous to that described above, although the energy scales and lengths are entirely different. The short-range binding of the α particle is due to the strong interaction and at large distances the electrostatic repulsion between the residual nucleus and the α particle dominates.

Multiply charged anions are well known in solids and solutions. The question whether small multiply charged anions exist as free entities, i.e., in the gas phase, and what electronic and structural properties they may exhibit has attracted attention for a long time. New experimental techniques and theoretical considerations have made the discovery of various kinds of free multiply charged anions possible and created an attractive and active field of research [2–11]

In the context of multiply charged anions, the RCB appeared in the literature for the first time when Compton and others examined multiply charged fullerene anions [12,13,3,14,15]. Although the theoretically predicted values for the electron affinity of ${C_{60}}^{-}$ have negative values [14–17], i.e., ${C_{60}}^{-}$ cannot bind a second electron, ${C_{60}}^{2-}$ has been found to be a long-lived gas-phase dianion with a lifetime longer than 10^{-3} s [18–20]. This inconsistency between experiment and theory could be qualitatively explained by the existence of the repulsive Coulomb barrier, which the outgoing electron has to pass during its emission. In the case of the fullerene dianion the energy of the electron lies above the threshold for detachment but far below the top of the RCB; thus detachment of this electron embodies an unlikely tunneling process. The fullerene ${C_{60}}^{2-}$ is therefore a metastable long-lived dianion.

Recently, very important and fundamental progress in the experimental examination of multiply charged anions was made by Wang, Ding, and Wang, who managed to measure the first photoelectron spectra (PES) of multiply charged an-

*Email address: andreas.dreuw@tc.pci.uni-heidelberg.de

ions. They used the electrospray ionization technique to generate the free anions, and after mass selection the negative ions were intercepted by a laser beam, and the kinetic energy of the photodetached electron was measured with a magnetic-bottle photoelectron analyzer [21]. Using this new technique, they investigated, for example, dicarboxylate dianions $^{-}OOC—(CH_2)_n—COO^{-}$ $(n=2-6)$ [22–24], $ML_6{}^{2-}$ dianions ($M=$ Re, Os, Ir, Pt; $L=$ Cl, Br) [25], and the tetra-anion of copper pthalocyanine tetrasulfonate [26,27]. When examining the PES of the copper pthalocyanine tetrasulfonate tetra-anion, Wang *et al.* observed a negative binding energy of the excess electrons, i.e., they measured photodetached electrons with higher kinetic energy than the energy of the laser beam. This observation is a direct experimental proof of the existence of the RCB, since the excess electrons of the tetra-anion are unbound but metastable with respect to emission. Their emission is hindered by the repulsive Coulomb barrier. A similar observation of a negative binding energy may of course also be possible when the PES of the above described fullerene dianion is measured.

From a theoretical point of view, the appearance of the RCB is clearly dominated by the electrostatic interaction between the outgoing electron and the residual anion. Nevertheless, the exact RCB is, in analogy to scattering potentials, a nonlocal energy-dependent potential, and, for this reason, neither straightforward to compute nor depictable in nature. The aim of this work is to illuminate the nature of the repulsive Coulomb barrier of multiply charged anions, to discuss its general appearance, and to introduce *ab initio* calculation schemes, which allow computation of local approximations of the exact RCB.

This paper is organized as follows. In Sec. II we outline the theory of the RCB, where we first consider the interaction energy between a point charge and a charged model sphere to illustrate the qualitative arguments made above for the existence of the RCB. Then we present an exact theory for the RCB, which is based on the Green's-function formalism. In the subsequent subsections we introduce local approximation schemes with the help of which one can straightforwardly compute energy-independent local RCB potentials. A theoretical analysis of these potentials is given in terms of multichannel scattering of distinguishable particles. These local approximation schemes are used in Sec. III to calculate the repulsive Coulomb barrier of atomic and molecular dianions. We focus here on the atomic dianions of fluorine and oxygen as well as on the molecular dianions of the linear carbon clusters $C_n{}^{2-}$ $(n=2,4,6,8)$. Furthermore, we make use of the computed *ab initio* RCB potentials to estimate the lifetimes of the metastable species.

II. THEORY OF THE REPULSIVE COULOMB BARRIER POTENTIAL

A. Preliminary considerations

In the Introduction we rationalized the existence of the RCB by considering the electrostatic forces that an electron experiences when it is emitted from a multiply charged anion or, equivalently, scattered from an anion. These forces are long-range repulsion and short-range attraction, combining to the repulsive Coulomb barrier. To corroborate these simple qualitative arguments and to get an idea of the height, width, and shape of the RCB we first examine the interaction energy between a negative point charge and an N-fold negatively charged sphere, the center of which is Z-fold positively charged $(N>Z)$. This primitive model system roughly reflects the electrostatic characteristics of the electron-anion system described above, especially when the target anion is atomic.

The interaction potential between a negative point charge and this model sphere is given by

$$V(r)=-\frac{Z}{r}+\int\frac{\rho(r')}{|r-r'|}d^3r', \tag{1}$$

where the first term describes the electrostatic attraction between the point charge and the Z-fold positively charged nucleus of the sphere, while the second is the interaction energy between the point charge and the exact charge distribution of the N negative charges of the sphere. Obviously, $V(r)$ depends on the choice of the charge distribution, and there are several possibilities to model a distribution, but here we concentrate on the following two.

The first model is a ''hard'' sphere in which the N negative charges are homogeneously distributed over the volume of a sphere with radius R. Its charge distribution $\rho_h(r)$ reads

$$\rho_h(r)=\frac{3N}{4\pi R^3}\Theta(R-r), \tag{2a}$$

where $\Theta(R-r)$ is the well-known step function.

A second and more realistic model for the charge distribution is a ''soft'' sphere, where the charge distribution decreases exponentially. This charge distribution $\rho_s(r)$ is given by

$$\rho_s(r)=\frac{N}{8\pi\alpha^3}\exp\left(-\frac{r}{\alpha}\right). \tag{2b}$$

Here, α represents a strength parameter of the exponential decrease of the charge. Substituting these two equations (2a) and (2b) into Eq. (1) and solving the integration, one readily obtains the potentials experienced by the point charge in both model cases. They are

$$V_h(r)=\begin{cases}\dfrac{N-Z}{r}, & r\geqslant R\\ -\dfrac{Z}{r}-\dfrac{N}{2R}\left(\dfrac{r}{R}\right)^2+\dfrac{3N}{2R}, & r\leqslant R\end{cases} \tag{3a}$$

for the hard-sphere case and

$$V_s(r)=\frac{N-Z}{r}-N\exp\left(-\frac{r}{\alpha}\right)\left\{\frac{1}{r}+\frac{1}{2\alpha}\right\} \tag{3b}$$

for the soft-sphere case.

To plot these analytical potentials we have chosen $Z=8$ and $N=9$, which are the nuclear charge and electron number of an oxygen anion. The potentials that we obtain are then

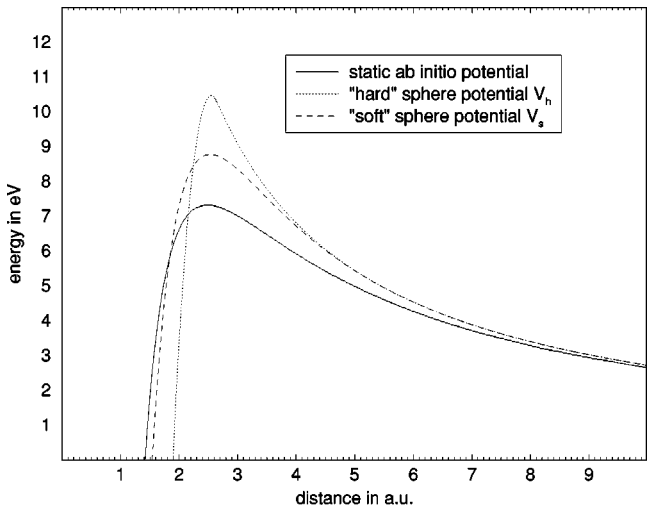

FIG. 1. Analytical RCB potentials of the hard- and soft-sphere models for O^{2-} are shown together with the *ab initio* local static RCB potential of O^{2-} (obtained with the local static approach at the level of the coupled-cluster singles plus doubles method; see Sec. III). The zero point of the energy scale corresponds to the energy of the free monoanion O^{-}.

approximate pictures of the RCB for detaching an electron from an atomic oxygen dianion. Furthermore, we have taken R as the experimental value of the radius of O^{2-}, which is known from crystallography to be 140 pm, i.e., 2.65 a.u. (atomic units). Introducing this radius R into the hard-sphere model and adjusting the strength parameter of the soft-sphere model, α, such that the maxima of both potentials are at the same position, one obtains the potentials shown in Fig. 1. The model potentials $V_h(r)$ and $V_s(r)$ are plotted together with the local static *ab initio* RCB of O^{2-}, which will be introduced later and discussed in detail in Secs. II C and III A.

While the positions of the maxima of the model potentials and of the *ab initio* static potential are in good agreement, the barrier heights are markedly different. It is clear that the barrier of the hard-sphere model must be higher than the barrier of the soft-sphere model, since the negative charges are strongly localized around the nucleus in the case of the hard sphere. Thus, the attraction of the nucleus is shielded more strongly by the negative charges of the hard sphere than by the soft sphere. The barrier height of the static *ab initio* potential is even smaller than that of the soft-sphere model due to the great diffuseness of the charge distribution of the oxygen anion.

Summarizing our short preliminary considerations, we have obtained analytical expressions for the interaction energy of a negative point charge with a charged sphere. These potentials are only simple approximations of the RCB in multiply charged anions, but give us an idea of the height and width that we have to expect when we investigate the RCB using *ab initio* approaches.

B. The exact potential

Green's functions (GF's) provide powerful tools to investigate properties of many- and several-body systems [28–30]. Numerous successful applications have been performed for solids [31,32], nuclei [33,34], and atoms, molecules, and clusters [35–39]. In connection with scattering theory, a particularly useful result has been obtained for the one-particle Green's function, which is the simplest in the hierarchy of the Green's functions. The kernel of this function (see below) is an *exact* one-particle potential for a scattering electron [40]. As we have argued in the Introduction, the RCB can also be seen as the potential that an electron experiences when it is scattered from a negatively charged target. For this reason, we can use the one-particle Green's function to evaluate the RCB.

The Green's functions are defined as the N-electron ground-state expectation values of a time-ordered product of creation and annihilation operators. The one-particle GF that describes an elastic scattering process reads

$$G_{\alpha\beta}(t,t') \equiv -i\langle \Psi_0^N | T\{b_\alpha(t) b_\beta^\dagger(t')\} | \Psi_0^N \rangle, \tag{4}$$

where Ψ_0^N is the exact N-electron ground state of the target, $b_\alpha(t)$ and $b_\beta^\dagger(t')$ denote annihilation and creation operators for projectiles in projectile states φ_α and φ_β, respectively, and T represents Wick's time-ordering operator [28,29]. This one-particle GF is subject to the well-known Dyson equation, which after Fourier transformation from time into energy space reads in matrix notation

$$\mathbf{G}(E) = \mathbf{G}^{(0)}(E) + \mathbf{G}^{(0)}(E)\boldsymbol{\Sigma}(E)\mathbf{G}(E). \tag{5}$$

Here, $\mathbf{G}^{(0)}(E)$ is the GF calculated with the unperturbed Hamiltonian, i.e., the Hamiltonian without particle-target interaction. E is the energy of the scattering system. The Dyson equation (5) relates the GF's for inelastic scattering $\mathbf{G}(E)$ to the free GF's via its kernel $\boldsymbol{\Sigma}(E)$, which is called the self-energy. The Dyson equation can be formally solved exactly by inversion, giving

$$\mathbf{G}(E) = [E\mathbf{1} - \mathbf{e} - \boldsymbol{\Sigma}(E)]^{-1}. \tag{6}$$

The unit matrix **1**, the diagonal matrix of projectile energies, **e**, and $\boldsymbol{\Sigma}(E)$ are matrices in projectile space.

The self-energy represents an effective, in general complex, energy-dependent one-particle potential caused by correlation effects [40]. If we neglect these correlation effects, the self-energy reduces to the well-known static-exchange potential [41] evaluated with respect to the Hartree-Fock (HF) potential. The self-energy consists of a static part $\Sigma(\infty)$ not depending on E and a dynamic part depending on E [38]:

$$\Sigma(E) = \Sigma(\infty) + M(E). \tag{7}$$

The static part has a simple interpretation. In spatial representation it can be written as

$$\Sigma(r,r',\infty) = W + \delta(r-r') \int \frac{\rho(\vec{r},\vec{r})}{|r-\vec{r}|} d\vec{r} - \frac{\rho(r,r')}{|r-r'|}, \tag{8}$$

where ρ is the exact one-particle density of the ground state of the target (here, of the anion) and W is the interaction potential of the projectile with the nuclei. The static part can thus be seen as the static-exchange interaction of the incom-

ing electron with the *correlated* target. An analysis of the physical origin of the dynamic part of the self-energy has been given in Ref. [42]. The self-energy $\Sigma(E)$ represents the exact potential experienced by a projectile, e.g., an electron, when it is elastically scattered from a target, e.g., an anion. All inelastic scattering channels are contained in the elastic $\Sigma(E)$ by losses of the elastic scattering cross section [43]. In the case of anionic targets we can obviously identify the self-energy with the repulsive Coulomb barrier. Applications of the self-energy to scattering of electrons by neutral molecules can be found in Refs. [44–46].

In conclusion, there exists an exact theory for the RCB based on the one-particle Green's functions. Unfortunately, the exact self-energy, i.e., an exact RCB, is not straightforward to compute. Furthermore, $\Sigma(E)$ is energy dependent, nonlocal, and probably complex, and, for these reasons, not easily depictable. Calculations of $\Sigma(E)$ are, of course, desirable, but out of range at the moment. Since we want to illustrate here the nature of the RCB and make systematic *ab initio* calculations, we have to introduce some approximations to circumvent the energy dependence and the nonlocal character of the RCB.

C. Local approximations of the RCB potentials

In this section we discuss three local approximation schemes with the help of which one can easily compute approximate *ab initio* RCB potentials. Two of these schemes have been introduced very recently and applied to compute the RCB of the dianion BeC_4^{2-} [47]. See also an application of the second scheme to the metastable $PtCl_4^{2-}$ dianion in [11]. All three schemes possess the great advantage of yielding local potentials that are depictable. These local potentials will help us to get a better understanding of the nature of the repulsive Coulomb barrier.

In the first approach, the RCB is calculated directly by using the Hartree-Fock ground-state wave function of the dianion. Let the dianion have $N+1$ electrons. We use the molecular orbitals of the dianion and take out one electron from the highest occupied orbital, the orbital from which the electron is emitted. Then we calculate the electrostatic potential by summing up the nucleus-electron attraction and electron-electron repulsion via

$$V_{\mathrm{DFOSA}}(r) = -\sum_{a=1}^{K} \frac{Z_a}{|r-R_a|} + \sum_{i=1}^{N} \int \frac{\phi_i^* \phi_i}{|r-r_i|} d\tau. \qquad (9)$$

In this equation the first term of the right-hand side describes the electrostatic attraction between K nuclei and the outgoing electron while the second term corresponds to the electrostatic repulsion between the outgoing electron and the N remaining electrons in the molecular orbitals of the dianion. Using this approach, we make several approximations. We circumvent the energy dependence of the exact RCB by formally setting the energy of the outgoing electron to the negative of the electron detachment energy. Furthermore, we neglect the exchange interaction between the outgoing electron and those of the residual anion. Since we use the molecular orbitals of the dianion, which do not interfer with the emitted electron, we call this method of calculating the RCB the *dianion-frozen-orbital static approach* (DFOSA). This approach is closely related to the static approximation without exchange and polarization, which is widely used in scattering theory. Strictly speaking, if we used in Eq. (9) the optimized orbitals of the monoanion instead of those of the dianion, we would exactly make such a static calculation for the scattering of an electron from the corresponding monoanion.

A second possibility for calculating the RCB in a straightforward and natural way is to compute the total energy of the monoanion in the presence of a negative point charge, which may represent the outgoing electron. If the negative point charge is placed at varying distances r from the monoanion, one readily obtains a complete potential-energy surface, which reflects the repulsive Coulomb barrier. The RCB is then given by the simple equation

$$V_{\mathrm{PCM}}(r) = E_0(r) - E_0. \qquad (10)$$

Here, $E_0(r)$ corresponds to the total energy of the monoanion in the presence of the negative point charge at the distance r, while E_0 is the total energy of the free monoanion, i.e., in the absence of the negative point charge. Using this approach to calculate the RCB, one takes account of electron relaxation and can easily apply *ab initio* methods beyond Hartree-Fock. It is, for example, possible to use the coupled-cluster singles plus doubles (CCSD) method, which makes correlation between the N electrons of the monoanion accessible. Furthermore, the exchange energy between these N electrons is also taken into account. On these grounds, it is clear that the N-electron system is described correctly by the point-charge model (PCM) at large distances between the point charge and the monoanion. The PCM reveals the correct shape of the RCB far away from the monoanion. At short distances this method, of course, possesses weaknesses (see also Sec. III A). For example, the monoanion is allowed to polarize statically when the electron approaches. If this is appropriate at all, it is only when the detaching electron moves very fast, which may not necessarily be correct. Thus, the quality of the RCB obtained can be poor at shorter distances.

Comparing the DFOSA method and the PCM, the latter reveals the correct shape of the RCB at large distances between the residual anion and the outgoing electron, because the anion is described correctly for this situation. The DFOSA yields a more reliable RCB in the inner region, when the detaching electron is close to the anion, since the orbitals of the dianion are used within the DFOSA approach. The two methods seem to complement one another to give a complete picture of the repulsive Coulomb barrier.

The third approach to the RCB consists of computing the local contribution of the static self-energy directly. Neglecting in Eqs. (7) and (8) the dynamic part and the exchange of the electron with the target anion, one obtains the *local static* potential

$$V_{\mathrm{LSA}}(r) = -\sum_{a=1}^{K} \frac{Z_a}{|r-R_a|} + \int \frac{\rho(\vec{r},\vec{r})}{|r-\vec{r}|} d\vec{r}. \qquad (11)$$

The one-particle density ρ of the anion can be computed with any *ab initio* method (see also Sec. II D 2). The response of the target's density to the projectile electron included in the PCM is, of course, absent in $V_{\mathrm{LSA}}(r)$. However, it will be shown below that the latter potential has advantages in that it does not suffer from some basic weaknesses of the other schemes.

Finally, we would like to mention that in all three local approaches discussed above the exchange interaction between the electron and the anion can, in principle, be taken into account by using local approximations like those used in density-functional theories. To be specific we have refrained from applying these approximations in the present work.

D. Analysis of the point-charge potential

In the following subsections, we analyze in detail the PCM discussed in the preceding subsection and outline its relation to multichannel Green's-function theory to obtain insight into the physical meaning of this attractive approach. Contact will be made with the local static potential. It will be shown how the latter can be computed with *ab initio* or other methods that do not provide the one-particle density ρ.

1. The point-charge matrix and point-charge potential

Within a local theory it is assumed that when an electron is emitted by a multiply charged anion, say a dianion, the Hamilton operator for the outgoing electron reads

$$H = h(r) + V(r), \tag{12}$$

where $h(r)$ represents the kinetic energy of the electron, and $V(r)$ is the potential that the electron experiences, which corresponds to the repulsive Coulomb barrier. In the point-charge model the RCB is calculated via the equation

$$V_{\mathrm{PCM}}(r) = E_0(r) - E_0$$

(see Sec. II C), where $E_0(r)$ denotes the energy of the monoanion in the presence of the point charge, while E_0 corresponds to the energy of the free monoanion. Multiplying by the ground-state wave function $|\Psi_0;r\rangle$ of the monoanion in the presence of the point charge at r from the right gives

$$V_{\mathrm{PCM}}(r)|\Psi_0;r\rangle = [E_0(r) - E_0]|\Psi_0;r\rangle. \tag{13}$$

Since $|\Psi_0;r\rangle$ obeys the Schrödinger equation

$$[H_T + v_{\mathrm{ele}}(r) + v_K(r)]|\Psi_0;r\rangle = E_0(r)|\Psi_0;r\rangle, \tag{14}$$

where H_T is the Hamiltonian of the target anion, one can use this equation to eliminate $E_0(r)$ in Eq. (13), which now takes on the following appearance:

$$V_{\mathrm{PCM}}(r)|\Psi_0;r\rangle = [H_T + v_{\mathrm{ele}}(r) + v_K(r) - E_0]|\Psi_0;r\rangle. \tag{15}$$

Here, $v_{\mathrm{ele}}(r)$ and $v_K(r)$ are the electrostatic interaction energies between the point charge at position r and the N electrons and K nuclei of the monoanion, respectively. They read

$$v_{\mathrm{ele}}(r) = \sum_{i=1}^{N} \frac{1}{|r_i - r|}, \quad v_K(r) = -\sum_{a=1}^{K} \frac{Z_a}{|R_a - r|}. \tag{16}$$

Expanding $|\Psi_0;r\rangle$ in the states $\{\Phi_j\}$ of the free monoanion, i.e., in the eigenstates of H_T,

$$|\Psi_0;r\rangle = \sum_j c_{j0}|\Phi_j\rangle, \tag{17}$$

and inserting into Eq. (15), we get

$$V_{\mathrm{PCM}}(r)\sum_j c_{j0}|\Phi_j\rangle = [H_T + u_{\mathrm{ele}}(r) + v_K(r) - E_0]\sum_j c_{j0}|\Phi_j\rangle. \tag{18}$$

By multiplying by $\langle\Phi_i|$ from the left and integrating over the target electrons, we obtain the matrix eigenvalue equation

$$(\mathbf{P} - V_{\mathrm{PCM}}\mathbf{1})\mathbf{c} = \mathbf{0} \tag{19}$$

for the eigenvalues $V_{\mathrm{PCM}}(r)$. Obviously, there is a point-charge potential associated with each of the target electronic states. In Eq. (19) **1** represents the unit matrix, **c** is the matrix of expansion coefficients, and the matrix elements of **P** are defined by

$$P_{ij}(r) = \langle\Phi_i|H_T + v_{\mathrm{ele}}(r) + v_K(r) - E_0|\Phi_j\rangle. \tag{20}$$

The matrix **P**, which we refer to as the point-charge matrix in the following, takes on the following appearance:

$$\mathbf{P} = \begin{pmatrix} A_{00} & A_{01} & A_{02} & \cdots & A_{0M} & \cdots \\ A_{10} & A_{11}+(E_1-E_0) & A_{12} & & & \\ A_{20} & A_{21} & A_{22}+(E_2-E_0) & & & \\ \vdots & & & \ddots & & \\ A_{M0} & & & & A_{MM}+(E_M-E_0) & \\ \vdots & & & & & \ddots \end{pmatrix}. \tag{21}$$

The point-charge matrix **P** can be split into two matrices,

$$\mathbf{P}=\mathbf{A}+\mathbf{E}. \tag{22}$$

E is a diagonal matrix with the elements E_i-E_0 along the diagonal, where E_i is the ith energy of the free anion. The matrix elements $A_{ij}(r)$ of the matrix **A** are defined as

$$A_{ij}(r)=\langle\Phi_i|v_{\mathrm{ele}}(r)+v_K(r)|\Phi_j\rangle. \tag{23}$$

The diagonal elements $A_{ii}(r)$ are the so-called local static potentials. $A_{ii}(r)$ is the interaction energy between a point charge and the exact charge density of the monoanion in the state Φ_i. In particular, $A_{00}(r)$ is identical with the local static potential introduced in the preceding subsection [see also Eq. (8)]: $V_{\mathrm{LSA}}(r)=A_{00}(r)$. These potentials correspond to the exact static potentials for scattering an electron from the monoanion, including the exchange and correlation of all electrons of the monoanion but without the exchange between the scattered electron and the target electrons.

When diagonalizing the point-charge matrix **P**, we obtain the eigenvalues $V_{\mathrm{PCM}}(r)$, which are the result of the point-charge model calculation, one RCB for each state of the monoanion. These potentials take account of the response of the monoanion on the presence of the point charge, i.e., the monoanion is allowed to polarize. The matrix **P** connects the static potentials to the point-charge model potentials.

2. The point-charge matrix and static potential

Evaluation of the static potentials is straightforward when the one-particle density of the target anion is known. However, this density is not explicitly available in some computer codes for *ab initio* methods beyond Hartree-Fock. One can easily circumvent this difficulty by a tricky modification of the point-charge model. When we do not use a full point charge in the PCM calculation but an infinitesimal point charge η, no response of the monoanion is expected. The interaction potential $V^{\eta}(r)$ between the infinitesimal point charge and the monoanion then reads

$$V^{\eta}(r)=\eta\left[\sum_{i=1}^{N}\frac{1}{|r_i-r|}-\sum_{a=1}^{K}\frac{Z_a}{|R_a-r|}\right]. \tag{24}$$

Thus, the point-charge matrix **P** takes on the following appearance [see Eq. (20)]:

$$\mathbf{P}^{\eta}=\begin{pmatrix} \eta A_{00} & \eta A_{01} & \eta A_{02} & \cdots \\ \sigma A_{10} & \eta A_{11}+(E_1-E_0) & \eta A_{12} & \\ \eta A_{20} & \eta A_{21} & \eta A_{22}+(E_2-E_0) & \\ \vdots & & & \ddots \end{pmatrix}. \tag{25}$$

Its eigenvalues can be evaluated using perturbation theory, and the first eigenvalue, for example, is given by

$$V^{\eta}_{\mathrm{PCM}}(r)=\eta A_{00}(r)+\eta^2\sum_{n}^{M}\frac{A_{0n}(r)A_{n0}(r)}{(E_n-E_0)}+O(\eta^3). \tag{26}$$

Dividing by η, the equation reads in the limit of $\eta\to 0$

$$\lim_{\eta\to 0}\frac{1}{\eta}V^{\eta}_{\mathrm{PCM}}(r)=A_{00}(r). \tag{27}$$

The local static potential $A_{00}(r)$, which describes the interaction between a full point charge at position r and the free monoanion in its ground state, can be calculated by performing a PCM calculation using an infinitesimal point charge. For brevity, we call this tricky modification of the point charge model the local static approach (LSA) in the following. This approach is of general applicability, since every electronic state of the target can be used in the calculation to generate the local static potential for the corresponding state. The infinitesimal point charge can be negative as well as positive, and every *ab initio* method that yields a total energy can be applied.

3. Relation to multichannel scattering Green's-function theory

In Sec. II B the one-particle Green's function for elastic scattering was introduced and an exact theory for the repulsive Coulomb barrier outlined. Since we use a point charge in the PCM to approximate the outgoing or, equivalently, the scattered electron, this ''electron'' is distinguishable from the electrons of the target. To analyze the PCM in terms of Green's functions, we have to compare the point-charge model with the Green's-function theory for scattering of nonelectronic particles from electronic targets [43], i.e., the scattered particle is distinguishable from the electrons of the target.

As usual, the total Hamiltonian for a scattering process reads

$$H=H_T+h+H_{TP}, \tag{28}$$

where H_T is the target (free monoanion) Hamiltonian, h represents the projectile Hamiltonian, and the interaction between projectile and target electrons is

$$H_{TP}=v_{\mathrm{ele}}(r)+v_K(r) \tag{29}$$

[see Eq. (16)]. Using this total Hamiltonian and the inelastic one-particle GF, it has been shown in Ref. [43] that a generalized Dyson equation can be obtained, which reads in matrix notation

$$\mathbf{G}(E)=\mathbf{G}^{(0)}(E)+\mathbf{G}^{(0)}(E)\mathbf{A}\mathbf{G}(E). \tag{30}$$

This generalized Dyson equation relates the inelastic GF's $\mathbf{G}(E)$ to the free GF's $\mathbf{G}^{(0)}(E)$ via a supermatrix **A**, which is given by

$$A_{ij}(r)=\langle\Phi_i|-\sum_{a=1}^{K}\frac{Z_a}{|R_a-r|}+\sum_{i=1}^{N}\frac{1}{|r_i-r|}|\Phi_j\rangle. \tag{31}$$

The scattering amplitudes $f_{jk}(r)$, which fully describe the inelastic scattering process $\Phi_k\to\Phi_j$, are given by the following set of equations:

$$\sum_j \{[E-h-(E_i-E_0)]\delta_{ij}-A_{ij}\}f_{jk}(r)=0, \qquad (32)$$

where E is the total energy of the projectile-plus-target system. In analogy to Eq. (19), this set of equations can be written as a matrix vector multiplication and takes on the following appearance:

$$(\mathbf{R}-\mathbf{1}E)\mathbf{F}=\mathbf{0}, \qquad (33)$$

where **1** is the unit matrix, **F** is the matrix of scattering amplitudes, and the elements of the matrix **R** are defined as

$$R_{ij}(r)=A_{ij}(r)+[h+(E_i-E_0)]\delta_{ij}. \qquad (34)$$

Equation (33) is an exact equation, i.e., its solutions are exact scattering amplitudes, which give exact elastic and inelastic scattering cross sections. Comparing the matrix **R** with the point-charge matrix **P** of Eq. (19), we easily see that these matrices are identical apart from h, which appears only in **R**. h represents the Hamiltonian of the projectile particle and, loosely speaking, corresponds to its kinetic energy. Setting h fomally equal to 0, i.e., neglecting the kinetic energy of the scattered electron, the matrix **R** is equal to the point-charge matrix **P**. We have thus shown that the PCM represents the adiabatic approximation of the exact theory for scattering a distinguishable particle from an electronic target. In reverse, the PCM can be used to calculate the eigenvalues and eigenstates of the exact multichannel matrix in the adiabatic approximation. Subsequently, the Hamiltonian h of the free particle can be added and a multichannel scattering calculation beyond the adiabatic approximation can be performed.

III. CALCULATION OF THE REPULSIVE COULOMB BARRIER POTENTIALS

In this section we present our results obtained from *ab initio* calculations on the repulsive Coulomb barrier of multiply charged anions. Here, we want to make first estimates of the barrier potentials in the framework of the local approximations introduced in the previous sections, although we know that the exact barrier potentials are nonlocal and energy dependent. As we have shown above, the exact potentials can be obtained with Green's-function methods, but these are, unfortunately, so far not straightforward to compute. For this reason, we use the DFOSA, the PCM, and the LSA introduced in Sec. II C and analyzed in Sec. II D to calculate the RCB's of various dianions.

Results on the atomic dianions F^{2-} and O^{2-} and on the linear series of the carbon cluster dianions C_n^{2-} ($n=2,4,6,8$) are shown. In Sec. III A we study the atomic dianions, discuss the basis-set dependence of the local approximation schemes, and outline their possible weaknesses. Section III B deals with the examination of the molecular C_n^{2-} dianions. There, we use the local RCB potentials to calculate detachment lifetimes for the carbon dianions in the framework of WKB theory.

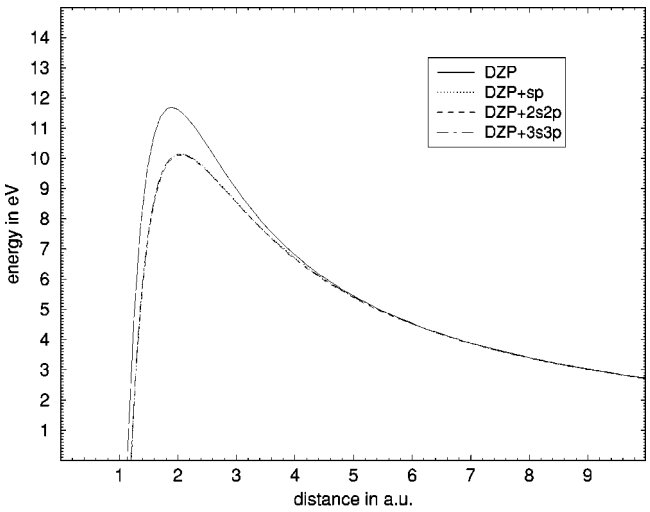

FIG. 2. Basis-set study of the local static RCB potentials of F^{2-} (upper part) and O^{2-} (lower part) obtained with the LSA. Both RCB potentials are essentially converged as a function of basis set when the DZP+sp basis set is used. The energy of the free monoanion is set to zero. Note that the angular momentum barrier has been added to the O^{2-} potentials (see text).

A. Atomic dianions and the induced electron detachment by the point charge

As a first step we have studied the RCB of the atomic dianions F^{2-} and O^{2-} with special emphasis on the basis-set dependence of the local approximation schemes. We have chosen atomic dianions merely as practical objects. The calculation times are short, and highly diffuse basis sets are easily employed.

We have computed the repulsive Coulomb barrier of the F^{2-} and O^{2-} dianions with the help of the DFOSA method at the level of restricted open-shell Hartree-Fock (ROHF) and restricted Hartree-Fock (RHF) approximations, respectively. The PCM and LSA calculations were performed using the coupled-cluster singles plus doubles method [48]. The basis-set dependence of the RCB of the dianions was checked by starting with the standard double-zeta plus polarization (DZP) basis set comprising Dunning's [49] contractions of Huzinaga's primitive sets [50], which were gradually augmented with one (DZP+sp), two (DZP+$2s2p$) and three (DZP+$3s3p$) sets of diffuse s- and p-type functions. The initial exponents for the diffuse s- and p-type functions for fluorine were 0.085 and 0.074, respectively, and 0.068 and 0.045 for oxygen. The second and third sets of diffuse functions where added in accord with the even scaling rule [51]. The use of basis sets of triple-zeta quality is not necessary, since their effect on the RCB is negligible.

The local static RCB potentials obtained using the local static approach as described in Sec. II C are displayed in Fig. 2. To plot the actually three-dimensional spherically symmetric potentials in one dimension, one has to respect the angular momentum of the outgoing electron. Since the outgoing electron from the O^{2-} dianion is a p electron, one has to add the angular momentum barrier to the RCB potential to obtain the correct one-dimensional RCB plot. For the fluorine dianion there exists no angular momentum barrier, as

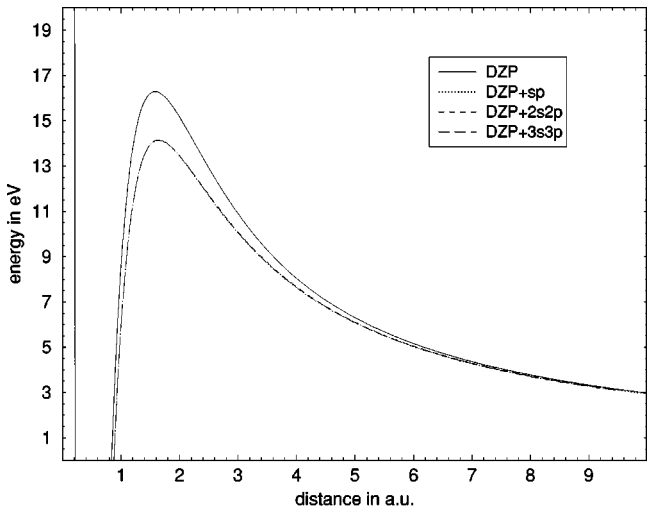

FIG. 3. Basis-set study of the RCB potentials of F^{2-} (upper part) and O^{2-} (lower part) obtained with the PCM. The RCB gradually decreases with increasing diffuseness of the basis set within the PCM calculations, i.e., the PCM is strongly basis-set dependent.

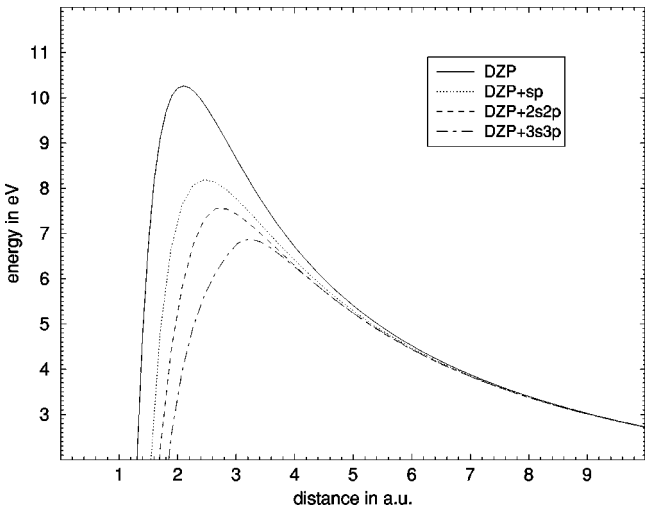

FIG. 4. Basis-set study of the DFOSA potentials of F^{2-} (upper part) and O^{2-} (lower part). While the F^{2-} potentials converge to the local static RCB with increasing diffuseness of the basis set, the RCB of O^{2-} vanishes.

the outgoing electron is an *s* electron.

One can see in Fig. 2 that the static potentials for F^{2-} and O^{2-} have already essentially converged as a function of basis set when the DZP+*sp* basis set is used. From a theoretical point of view, the local static RCB potential has to be basis-set independent once the target anion is properly described, because the static RCB depends only on the charge distribution of the target anion [see Eq. (11) in Sec. II C). Obviously, this is already the case for these atomic dianions when the DZP+*sp* basis set is used.

In Fig. 3 the RCB potentials for F^{2-} and O^{2-} are displayed as calculated with the point-charge model. The RCB's of both atomic dianions decrease with increasing diffuseness of the basis sets and seem to disappear in the limit of an infinite basis set. In the PCM a negative point charge is brought up to the target anion, and for this reason the height and width of the RCB are determined by the ability of the system to react to the presence of the point charge. When an electron approaches an anion, the target anion polarizes and a weakly bound anion may also be ionized. Due to the strong electrostatic repulsion between the point charge and the extra electron of the anionic target, electron detachment of the anionic target electron is *always* induced within a PCM calculation below some position *r* of the point charge. This is, of course, physically not correct and is the major weakness of the point-charge model.

To make this induced electron detachment by the point charge clearer, we consider the PCM calculation for O^- as the target. O^- possesses a bound $^2P_{3/2}$ ground state that has an electron detachment energy (EDE) of 1.461 eV [52]. When a point charge approaches the O^- ground state, the state becomes unbound due to the electrostatic repulsion between the excess electron of the anionic target and the point charge. This happens when the Coulomb repulsion is larger than the binding energy of the electron. For the oxygen anion this is the case when the distance between anion and point charge is smaller than about 10 Å, according to $r \leqslant 14.395/(\mathrm{EDE})$, where *r* is given in Å and EDE in eV. Clearly, we detach the excess electron of O^- by approaching it with the point charge. The detachment of O^- can be ''observed'' during a PCM calculation at the Hartree-Fock level in the orbital energy of the anionic electron. When the point charge is farther away than 10 Å, the orbital energy is negative, i.e., the electron is bound, and when the distance becomes shorter, the orbital energy becomes positive, i.e., the electron is unbound. This induced electron detachment is the major weakness of the point-charge model, because, independently of how strongly the anionic electron is bound, i.e., what kind of system we examine, the detachment of the anionic electron is always induced when the point charge is spatially close enough to the anionic target. Then the anion–point-charge system represents an unbound resonance state. Returning to the basis-set dependence of this model, it is now clear that the height of the barrier decreases as the basis set describes this unbound resonance state in more detail, i.e., as the basis set becomes more diffuse.

Finally, we have examined the basis-set dependence of the DFOSA method, and the DFOSA potentials that were obtained for F^{2-} and O^{2-} are displayed in Fig. 4. The RCB of F^{2-} decreases markedly when the first set of diffuse functions is added, but increases again with the addition of the second and third sets. This behavior of the RCB can be understood when one analyzes the DFOSA method and the F^{2-} dianion. In a DFOSA calculation like that described in Sec. II C, we use the Hartree-Fock orbitals of the dianion to sum up the electron-electron repulsion and the nucleus-electron attraction. The Hartree-Fock orbitals are generated in the framework of the ROHF method, because F^{2-} is an open-shell system. When the unbound F^{2-} dianion is calculated with the bound-state ROHF method and the basis set employed is getting more and more diffuse, the method tends to describe a bound F^- anion and an unbound electron. Hypothetically, using an infinite basis set, we would get the exact HF orbitals of F^- and an unbound electron with zero kinetic

energy. Using these orbitals of the monoanion, i.e., its correct one-particle density at the Hartree-Fock level in the DFOSA calculation, we would, of course, obtain the local static RCB at the theoretical level of HF. That means that the RCB of an open-shell multiply charged anion calculated with the DFOSA method converges toward the local static RCB with increasing diffuseness of the basis set.

In contrast to that of the open-shell F^{2-} dianion, the RCB of the closed-shell O^{2-} dianion vanishes (Fig. 4) in the framework of the DFOSA, when more and more diffuse basis sets are used. Again, we describe an unbound resonance state with the bound-state RHF method. Because the RHF method treats electrons with α and β spins equally, i.e., all orbitals are doubly occupied, the bound-state calculation can converge only to solutions in which electron pairs are retained. Therefore, the solution of the RHF calculation for O^{2-} using an infinite basis set can only be a neutral O atom and two unbound electrons with zero kinetic energy. Consequently, the RCB disappears when we use these orbitals in the DFOSA calculation.

Summarizing the basis-set dependence of the local approximations, only the LSA is basis-set independent, once the basis set is sufficiently large to appropriately describe the anionic target. The PCM and the DFOSA methods are strongly basis-set dependent, since within these schemes unbound states are calculated with bound-state methods. On these grounds, the use of the PCM and the DFOSA methods makes sense only when not too diffuse basis sets are employed. A good choice of the basis set is of general importance in any quantum-chemical calculation, and thus one has to define a basis-set selection criterion for the approximation schemes. The only reasonable criterion is the basis-set independence of the local static approach. For this reason, the first basis set for which the local static approach is converged should be the basis set in all further RCB calculations. Here, it was the DZP+sp basis set, since this is the smallest basis set for which the local static RCB's of F^{2-} and O^{2-} converged (see Fig. 2).

To apply the local approximation schemes successfully one has to reflect the underlying approximations and the systems that are to be examined with these methods. Because we neglect exchange between the extra electron and the target (monoanion) in all three schemes and exchange is important for spatially small atomic systems, we may not expect quantitative accuracy in our calculations on atomic dianions. But nonetheless atoms are reasonable objects for studying the weaknesses and the limits of applicability of the local approximation schemes. Furthermore, we may suggest the use of density-functional theory (DFT) within the models, because exchange is approximately contained in the DFT method.

In view of the above findings concerning the PCM and DFOSA, one may ask whether these physically appealing methods make any sense at all. As discussed above, the system can be viewed as in an unbound resonance state and several techniques are available to compute such resonances [53–55]. By analytic continuation into the complex energy plane, the energy of the resonance becomes $E_{\mathrm{res}}=E_r - i\Gamma/2$, where E_r is the real part of the resonance energy and Γ the decay width ($\tau=\hbar/\Gamma$ is the lifetime of the resonance) [53,54]. In the present context the appropriate technique will lead to complex DFOSA and PCM potentials to take account of the possible losses due to the induced ionization by the point charge. Another possibility is to view the resonance as a discrete state embedded in the continuum. This discrete state can be computed using stabilization techniques employing compact basis sets [55]. In the present context the scheme for choosing an appropriate compact basis set for DFOSA and PCM calculations is in line with the stabilization technique.

B. Molecular dianions: C_n^{2-} ($n=2,4,6,8$)

In the previous subsection we saw that exchange is important for spatially small atomic systems and, since exchange is neglected in the local approximation schemes, the RCB's obtained provide only crude estimates of the ''true'' RCB's. In this subsection we turn to the examination of molecular dianions. These systems are more extended and exchange plays a minor role, and we expect that the use of the local approximation schemes will yield reliable RCB's here.

We have examined the repulsive Coulomb barrier of the linear carbon dianions C_n^{2-} ($n=2,4,6,8$), of which C_8^{2-} was observed experimentally in 1990 by Schauer *et al.* [56]. We chose these dianions for two reasons. On the one hand, they are experimentally and theoretically well studied and ample data are available in the literature [57,39,58,59]. On the other hand, there is still a puzzle concerning C_8^{2-}. Although the peak of C_8^{2-} is one of the most abundant in the mass spectrum of the carbon dianions, it has been found to be adiabatically unstable with respect to electron emission by about 0.1 eV [57]. In contrast, C_7^{2-}, which is the smallest observed carbon dianion, possesses a D_{3h} starlike structure and is electronically stable [58,59], but its peak in the mass spectrum is less intense than that of C_8^{2-}.

The RCB potentials of the linear carbon dianions have been calculated using all three methods discussed in Sec. II C. The PCM and LSA were employed at the CCSD level and DFOSA at the level of restricted Hartree-Fock. All geometries of the carbon dianions examined were optimized at the CCSD level using the DZP+sp basis set and were held fixed in the RCB calculations. In analogy to the case of atomic dianions (Sec. III A), we checked the basis-set dependence of the RCB of the molecular dianions. As an example, we computed the RCB of C_4^{2-} using all three local approximation schemes starting with the DZP basis set. The basis set was then gradually augmented with one (DZP+sp) and two (DZP+$2s2p$) sets of diffuse s- and p-type functions, the exponents of which were 0.040 893 and 0.027 188, respectively.

As for the atomic dianions, the local static approach is already converged when the DZP+sp basis set is used, i.e., the monoanion is appropriately described by this basis set. The DZP+sp basis is therefore chosen to be the standard basis set for calculations of the RCB's of all carbon dianions examined. As expected, the RCB of the closed-shell C_4^{2-} gradually decreases when the DFOSA method and the point-charge model are applied and more and more diffuse basis

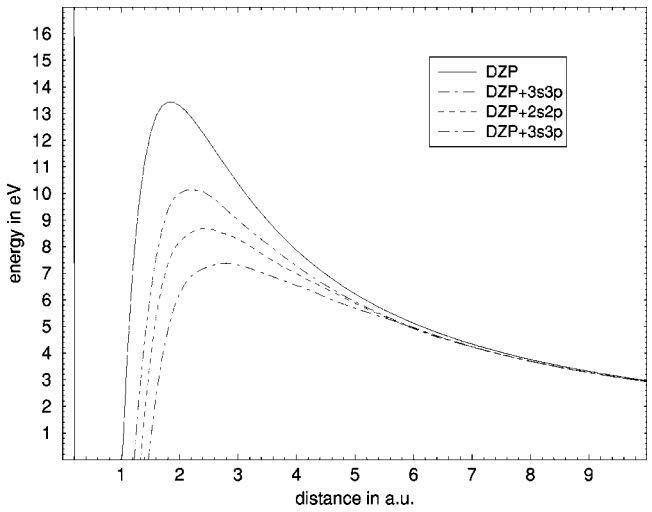

FIG. 5. Two-dimensional picture of the RCB of C_6^{2-} calculated in the framework of the DFOSA. The potential is strongly anisotropic, and as one can easily see the minimum-energy path for electron emission from the dianion is along the horizontal mirror plane of the $D_{\infty h}$ symmetric dianion. Contour lines are projected on the *xy* plane for several heights of the barrier (see legend). The energy is given in eV, and the lengths are given in angstrŏms.

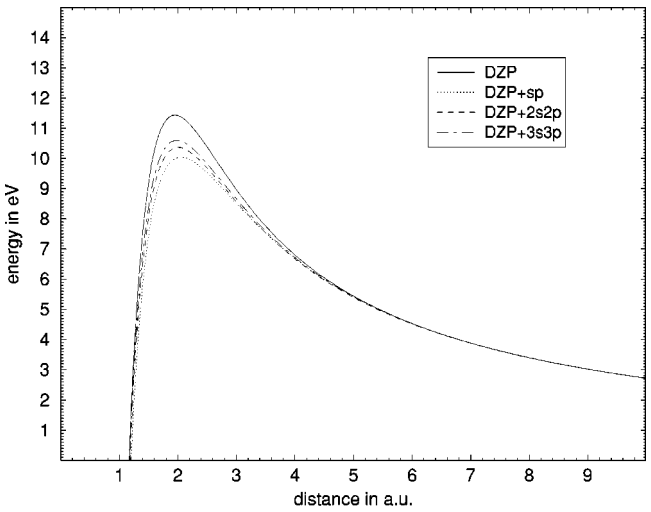

FIG. 6. Comparison of the RCB potentials of the linear carbon dianions C_n^{2-} $(n=2,4,6,8)$ along the minimum-energy path for electron emission calculated with the DFOSA method using the DZP+*sp* basis set. The vertical electron detachment energies of the dianions computed at the level of CCSD/(DZP+*sp*) are indicated by horizontal bars, on which the corresponding calculated lifetimes for *vertical* electron detachment of the respective dianions are given in seconds. The lifetimes have been calculated in the framework of semiclassical WKB theory (see text). The zero point of the energy scale corresponds to the energy of the respective monoanions.

sets are used. It is worth noting that the basis-set dependence of these local approximation schemes is much less significant for the molecular C_4^{2-} than for the atoms. While the RCB of O^{2-} decreased by about 5 and 3.5 eV in the DFOSA and PCM calculations, respectively, when going from the DZP to the DZP+*sp* basis set, the decrease is only 0.55 and 0.3 eV for C_4^{2-}. This makes us confident of obtaining reliable potentials for extended systems like molecular dianions with the help of local calculation schemes.

The RCB potentials are, of course, three dimensional, but rotationally symmetric for the linear C_n^{2-} dianions. For illustration, a two-dimensional picture of the RCB of C_6^{2-} obtained using the DFOSA method is shown in Fig. 5. The RCB is highly anisotropic. The maxima of the potential are at the ends of the C_6^{2-} molecule, where the excess charges are located. The minima are placed along the horizontal mirror plane of the molecule. These minima correspond to the minimum-energy path for electron emission from the C_6^{2-} dianion. The RCB's of all linear even-numbered carbon dianions possess this typical shape, but the shorter the chain length the higher is the RCB in all directions, due to the increased electrostatic repulsion between the excess charges. A comparison of the RCB potentials of the linear carbon cluster dianions along the minimum-energy path for electron emission is shown in Fig. 6. These potentials have been calculated with the DFOSA method using the DZP+*sp* basis set. As expected, the height of the RCB decreases systematically with the size of the system. We find a decrease by about 2.5 eV from C_2^{2-} to C_8^{2-}.

We have used the RCB potentials of the carbon dianions to calculate the tunneling probability and the lifetime of these systems in the framework of semiclassical WKB theory. The tunneling probability is given by the formula

$$P=\exp\left(-\frac{2}{\hbar}\int_{r_1}^{r_2}\sqrt{2m[E-V(r)]}dr\right),$$

where E is the energy of the electron, $V(r)$ the RCB, and r_1 and r_2 define the width of the barrier at energy E. The lifetime of the dianion can finally be calculated using the formula

$$\tau=\frac{2\pi}{P\omega},$$

where ω is the frequency with which the electron hits the RCB. This frequency can be obtained by solving the equation of motion for the electron with the assumption that the potential in the inner region is dominated by the electrostatic attraction between the nucleus and the outgoing electron, i.e., the potential has the shape of r^{-1}. The use of this semiclassical approach is limited to one-dimensional potentials and actually the RCB is, as already mentioned, three dimensional. We solve this conceptual problem by assuming that the electron leaves the dianion via the minimum-energy path outlined above. A three-dimensional calculation of the lifetime would be desirable to improve the reliability of the numbers, but this is beyond the scope of this work. Here, we are interested only in estimating the lifetimes and investigating their dependence on the chain size. A tedious three-dimensional calculation would certainly be justified when using a more accurate potential like the one discussed in Sec. II B.

To study the influence of the potential on the lifetime, i.e., how the lifetime depends on the approximation schemes

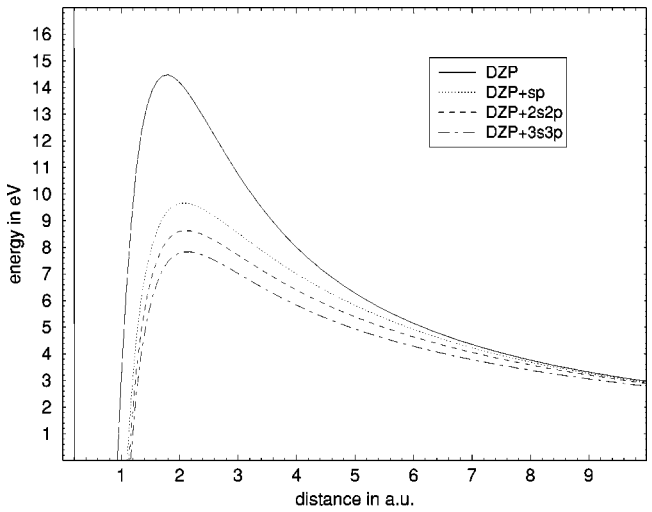

FIG. 7. In the upper part the computed lifetimes of the C_8^{2-} dianion are displayed as a function of the energy of the emitted electron. For the calculation of the lifetime we have used the LSA (full line), DFOSA (dotted line), and PCM (dashed line) potentials. These potentials are displayed in the lower part. Although the potentials are quite different, the computed lifetimes are quite similar and vary at most by a factor of 2. For electron energies below 0.35 eV (indicated by the horizontal line in the lower part) the lifetime of the C_8^{2-} dianion was found to be longer than 10^{-5} s for all three potentials. A lifetime of about 10^{-5} s is typically needed to observe a system in a mass spectrometer experiment.

used to compute the potential, we have calculated the lifetime of C_8^{2-} for energies between 0.1 and 2.0 eV using the LSA, DFOSA, and PCM potentials. The calculated lifetimes are displayed together with the corresponding potentials in Fig. 7. The investigation shows that the lifetime depends much more strongly on the energy of the outgoing electron than on the potential. Although the shapes of all three potentials are quite different, the results for the lifetime at a given energy are quite similar and vary at most by a factor of 2. It seems that the errors embodied in the different approximation schemes are canceling each other when calculating the lifetime. This encourages us to assume that the lifetimes obtained are more reliable than the potentials themselves. Furthermore, one can see that for electron energies below 0.35 eV, which corresponds to an electron detachment energy of -0.35 eV, the dianion lifetime is markedly longer than 10^{-5} s, which is the limit for experimental observation in a mass spectrometer.

Watts and Bartlett [57] found that the C_8^{2-} dianion is vertically stable with respect to electron emission but adiabatically unstable by about 0.1 eV. Assuming 0.1 eV to be the energy of the outgoing electron, we obtain a tunneling lifetime of about 2×10^{11} s for the C_8^{2-} system; thus no significant electronic decay should be observed in the experiment. Since the linear isomers of the carbon dianions are thermodynamically more stable than the branched isomers like, e.g., C_7^{2-}, it is now clear that the abundance of the peaks of C_7^{2-} and C_8^{2-} in the mass spectrum is determined by the thermodynamically determined generation rate and not by the electronic stability of these dianions.

For completeness, we have calculated the tunneling lifetimes for C_2^{2-}, C_4^{2-}, and C_6^{2-}. Since the specific local approximation scheme used plays only a minor role in determining the lifetime, we have used the DFOSA potential (Fig. 6). In contrast, the quality of the calculation of the energy of the outgoing electron is of great importance; thus we have used the vertical electron detachment energy calculated at the level of CCSD (DZP+sp) by subtracting the computed total energy of the dianion from that of the monoanion. These vertical detachment energies of C_2^{2-}, C_4^{2-}, and C_6^{2-} are -3.81, -2.12, and -0.77 eV, respectively. The corresponding vertical energy of C_8^{2-} has been calculated to be 0.33 eV at the CCSD level of theory, i.e., C_8^{2-} is stable with respect to vertical electron emission and has an infinite lifetime (in contrast to the case of adiabatic electron emission, see above). The lifetimes obtained for the linear carbon dianions for vertical electron emission are 9×10^{-15}, 1.5×10^{-13}, and 1.7×10^{-9} s for C_2^{2-}, C_4^{2-}, and C_6^{2-}, respectively. From that point of view, all three dianions are too short lived to be observable in a mass spectrometer, which is in agreement with the experiments.

IV. SUMMARY AND CONCLUSIONS

In this paper we have examined the repulsive Coulomb barrier for electron emission from multiply charged anions. The RCB is a general phenomenon in multiply charged anions: it arises due to the combination of long-range repulsion between the emitted electron and the residual anion and short-range attraction of the nucleus. Although the RCB is dominated by the electrostatic forces present, it is a nonlocal energy-dependent potential, which is neither easy to compute nor depictable in nature. Since the RCB is closely related to scattering potentials, there exists an exact theory for the RCB that is founded on the Green's-function formalism for scattering processes. We have shown that the RCB can be related to the self-energy $\Sigma(E)$. The self-energy is an optical potential connecting the Green's function for scattering with the free Green's function according to the well-known Dyson equation.

Since $\Sigma(E)$ is so far not straightforward to compute, we have introduced local approximation schemes. These are the dianion-frozen-orbital static approximation, the point-charge model, and the local static approach. In a DFOSA calculation, the nucleus-electron attraction and the electron-electron repulsion are summed up using the frozen orbitals of the dianion. In the PCM calculation a full point charge is brought up to the anion, and the total energies of the anion–point-charge system and the free anion are subtracted to obtain the RCB. In contrast, the local static potential is obtained as the interaction of a point charge with the correlated electron density of the anion. Technically, this potential can be obtained within the derived LSA. In the LSA method an infinitesimal point charge approaches the anion and afterward the potential obtained is scaled up to a full point charge.

A thorough theoretical analysis of the PCM and LSA methods has proved their relation to multichannel-scattering Green's-function theory. While the PCM represents an adia-

batic approximation to the exact theory of scattering a distinguishable particle from an electronic target, the LSA method yields the local static potential of the target anion, which corresponds to a diagonal element of the scattering matrix. These approaches are of general applicability since every *ab initio* method can be employed, including those methods that do not compute or do not explicitly provide the one-particle density of the monoanion.

We have applied the local approximation schemes to investigate atomic and molecular dianions. The atomic F^{2-} and O^{2-} dianions are reasonable objects to use to study the basis-set dependence of the local schemes. While the DFOSA and PCM potentials strongly depend on the basis set employed, the LSA has been found to be basis-set independent at sufficiently large basis sets. We have used the LSA to define a criterion for basis-set selection for the other methods. The smallest basis set for which the LSA converged is chosen to be the one used in all other local RCB calculations. This criterion as well as the behavior of the various potentials as a function of basis-set size are understood and discussed theoretically.

The atomic dianions serve merely as study objects. Since exchange between the electron and the target anion is neglected in the local schemes, and this interaction is important for the spatially compact atomic systems, the calculated RCB potentials for F^{2-} and O^{2-} are only crude estimates of the exact RCB. To remedy the situation we suggest using a local approximation to the exchange, as is common in DFT calculations.

Turning to larger systems, the underlying local approximations become less severe, since the exchange interaction of the electron with the extended target plays a less significant role. This makes us confident of obtaining local potentials that are more reliable estimates of the exact RCB. Examination of the RCB potentials of the linear carbon dianions C_n^{2-} $(n=2,4,6,8)$ has shown that the molecular DFOSA and PCM potentials are much less basis-set dependent than those of atomic systems. Not surprisingly, the repulsive Coulomb barrier decreases the larger the carbon dianion becomes, due to the decreasing electrostatic repulsion of the excess charges. This lowering of the barrier is accompanied, however, by an increase of the electron binding energy of the excess electron. Using the calculated RCB potentials we have estimated the lifetimes of the metastable carbon dianions with the help of semiclassical WKB theory. We have calculated the tunneling lifetime along the minimum-energy path for electron emission, which is along the horizontal mirror plane of the $D_{\infty h}$ symmetric systems. We have found that the lifetime for vertical electron emission grows markedly from 9×10^{-15} to 1.5×10^{-13} and 1.7×10^{-9} s when going from C_2^{2-} to C_4^{2-} and C_6^{2-}. The dianion C_8^{2-} is vertically stable, but adiabatically unstable. We have estimated its lifetime with respect to adiabatic electron emission to be very long $(2\times10^{11}\,\mathrm{s})$, however. On these grounds, only C_8^{2-} should be experimentally accessible in a mass spectrometer, and no relevant electronic decay should be observed. This is in agreement with the experimental findings.

ACKNOWLEDGMENTS

The authors would like to thank Professor Nimrod Moiseyev, Rainer Schork, and Alexander Thiel for helpful discussions. Computer time was generously provided by the Rechenzentrum der Universität Heidelberg.

[1] P. E. Hodgson, E. Gadioli, and E. G. Erba, *Introductory Nuclear Physics* (Oxford Science Publications, Oxford, 1997).
[2] J. Kalcher and A. F. Sax, Chem. Rev. **94**, 2291 (1994).
[3] M. K. Scheller, R. N. Compton, and L. S. Cederbaum, Science **270**, 1160 (1995).
[4] G. R. Freeman and N. H. March, J. Phys. Chem. **100**, 4331 (1996).
[5] L.-S. Wang and X.-B. Wang, J. Phys. Chem. **104**, 1978 (2000).
[6] J. Klein and R. Middleton, Nucl. Instrum. Methods Phys. Res. B **159**, 8 (1999).
[7] R. Middleton and J. Klein, Phys. Rev. A **60**, 3515 (1999).
[8] A. Dreuw, T. Sommerfeld, and L. S. Cederbaum, J. Chem. Phys. **109**, 2727 (1998).
[9] A. I. Boldyrev and J. Simons, J. Phys. Chem. **98**, 2298 (1994).
[10] H. Gnaser, Phys. Rev. A **60**, R2645 (1999).
[11] P. Weiss, O. Hampe, S. Gilb, and M. M. Kappes, Chem. Phys. Lett. **321**, 426 (2000).
[12] C. Jin, R. L. Hettich, R. N. Compton, A. Tuinman, A. Derecskei-Kovacs, D. S. Marynick, and B. I. Dunlap, Phys. Rev. Lett. **73**, 2821 (1994).
[13] R. N. Compton, A. A. Tuinman, C. E. Klots, M. R. Pederson, and D. C. Patton, Phys. Rev. Lett. **78**, 4367 (1997).
[14] R. L. Martin and J. P. Ritchie, Phys. Rev. B **48**, 4845 (1993).
[15] C. Yannouleas and U. Landmann, Chem. Phys. Lett. **217**, 396 (1994).
[16] A. H. H. Chang, W. C. Ermler, and R. Pitzer, J. Phys. Chem. **95**, 9288 (1991).
[17] M. R. Pederson and A. A. Quong, Phys. Rev. B **46**, 13 584 (1992).
[18] R. L. Hettlich, R. N. Compton, and R. H. Ritchie, Phys. Rev. Lett. **67**, 1242 (1991).
[19] P. A. Limbach, L. Schweikhard, K. A. Cowen, A. G. Marshall, M. T. M. Dermott, and J. V. Coe, J. Am. Chem. Soc. **113**, 6795 (1991).
[20] A. Mandelbaum and A. Etinger, Org. Mass Spectrom. **28**, 487 (1993).
[21] L.-S. Wang, C.-F. Ding, and X.-B. Wang, Rev. Sci. Instrum. **70**, 1957 (1999).
[22] L.-S. Wang, C.-F. Ding, X.-B. Wang, and J. B. Nicholas, Phys. Rev. Lett. **81**, 2667 (1998).
[23] C.-F. Ding, X.-B. Wang, and L.-S. Wang, J. Phys. Chem. **102**, 8633 (1998).
[24] X.-B. Wang, C.-F. Ding, and L.-S. Wang, Chem. Phys. Lett. **307**, 391 (1999).
[25] X.-B. Wang and L.-S. Wang, J. Chem. Phys. **111**, 4497 (1999).
[26] X.-B. Wang and L.-S. Wang, Nature (London) **400**, 245 (1999).

[27] X.-B. Wang, K. Ferris, and L.-S. Wang, J. Chem. Phys. **104**, 25 (2000).
[28] A. L. Fetter and J. D. Walecka, *Quantum Theory of Many-Particle Systems* (McGraw-Hill, New York, 1971).
[29] D. J. Thouless, *The Quantum Mechanics of Many Body Systems* (Academic, New York, 1972).
[30] R. D. Mattuck, *A Guide to Feynman Diagrams in the Many-Body Problem* (McGraw-Hill, New York, 1976).
[31] E. N. Economou, *Green's Functions in Quantum Physics* (Springer-Verlag, Heidelberg, 1979).
[32] G. D. Mahan, *Many-Particle Physics* (Plenum, New York, 1981).
[33] A. B. Migdal, *Theory of Finite Systems and Applications to Atomic Nuclei* (Wiley, New York, 1971).
[34] F. Capuzzi and C. Mahaux, Ann. Phys. (N.Y.) **239**, 57 (1995).
[35] J. Linderberg and Y. Ohrn, *Propagators in Quantum Chemistry* (Academic, New York, 1973).
[36] M. F. Hermann, K. F. Freed, and D. L. Yeager, Adv. Chem. Phys. **48**, 1 (1981).
[37] L. S. Cederbaum, W. Domcke, J. Schirmer, and W. von Niessen, Adv. Chem. Phys. **65**, 115 (1986).
[38] L. S. Cederbaum, in *The Encyclopedia of Computational Chemistry*, edited by P. v. R. Schleyer, N. L. Clark, J. Gasteiger, H. F. Schaefer III, and P. R. Schreiner (Wiley, Chichester, U.K., 1998).
[39] V. G. Zakrzewski and J. V. Ortiz, J. Chem. Phys. **102**, 294 (1995).
[40] J. S. Bell and E. J. Squires, Phys. Rev. Lett. **3**, 96 (1959).
[41] N. F. Lane, Rev. Mod. Phys. **52**, 29 (1980).
[42] H.-D. Meyer, J. Phys. B **21**, 3777 (1988).
[43] L. S. Cederbaum, Few-Body Syst. **21**, 211 (1996).
[44] A. Klonover and U. Kaldor, J. Phys. B **12**, 323 (1979).
[45] M. Berman, O. Walter, and L. S. Cederbaum, Phys. Rev. Lett. **50**, 1979 (1983).
[46] H.-D. Meyer, Phys. Rev. A **40**, 5605 (1989).
[47] A. Dreuw and L. S. Cederbaum, J. Chem. Phys. **112**, 7400 (2000).
[48] R. J. Bartlett, J. Phys. Chem. **93**, 1697 (1989).
[49] T. H. Dunning, Jr., J. Chem. Phys. **53**, 2823 (1970).
[50] S. Huzinaga, J. Chem. Phys. **42**, 1293 (1965).
[51] J. S. Binkley and J. A. Pople, Int. J. Quantum Chem. **9**, 229 (1975).
[52] H. Hotop and W. C. Lineberger, J. Phys. Chem. Ref. Data **14**, 731 (1985).
[53] N. Moiseyev, Phys. Rep. **302**, 211 (1998).
[54] U. V. Riss and H.-D. Meyer, J. Phys. B **26**, 4503 (1993).
[55] A. U. Hazi and H. S. Taylor, Phys. Rev. A **1**, 1109 (1970).
[56] S. N. Schauer, P. Williams, and R. N. Compton, Phys. Rev. Lett. **65**, 625 (1990).
[57] J. D. Watts and R. J. Bartlett, J. Chem. Phys. **97**, 3445 (1992).
[58] T. Sommerfeld, M. K. Scheller, and L. S. Cederbaum, Chem. Phys. Lett. **209**, 216 (1993).
[59] T. Sommerfeld, M. K. Scheller, and L. S. Cederbaum, J. Phys. Chem. **98**, 8914 (1994).